Analysis of Gas-fluidized Solid Systems by X-ray Absorption

E. W. Grohse

General Electric Company, Schenectady, New York

X-ray absorption is presented as a unique tool for the study of the fundamentals of gas fluidization. For example, bed-density profiles, valuable indexes of the quality of fluidization, are readily determined by means of X-ray absorption. No internal probes, to interfere with the normal action within a fluidized bed, are involved.

As an initial application of X-ray absorption to fluidization, the results of a study of the effect of mode of distribution of gas to a fluidized bed are presented. The importance of this variable, only superficially discussed in previous literature, is clearly shown by these results. Application of X-ray absorption to other chemical engineering operations is readily conceivable.

Although a considerable number of experimental investigations of gas-fluidized solid systems have been reported during the past 5 years or so, with notable exceptions these have been confined to the study of gross phenomena of fluidization. For example, over-all bed expansions and over-all coefficients of heat transfer between fluidized beds and confining surfaces have been rather profusely reported. On the other hand, very little study of local phenomena within fluidized beds has been reported. Furthermore, very little disclosure has appeared in the literature of the important effects of certain variables, such as mode of gas distribution to a bed of solids, upon the quality of fluidization produced.

A major deterrent in the advancement of fundamental knowledge in fluidization is presented by the lack of a reliable, comprehensive index of the quality of fluidization occurring in a given apparatus. Several indexes of quality of fluidization have been proposed (*2, 8, 10*), but none of these appear adequate for general use. Of those already proposed, the index of Morse and Ballou (*8*) holds the most promise, as its calculation is based upon the measurement of local phenomena within a fluidized bed. The correlation of this index, or of the measurements involved, with simultaneous measurements of heat and/or mass transfer between the fluidized solids and the fluidizing gas would be expected to lead to a superior, more nearly complete, index of the quality of performance of a fluidized bed.

This paper represents the initial report of a continuing investigation, the main goals of which are (1) development of fundamental information on the operation of gas-fluidized beds of solids, (2) study of the effects upon fluidization of variables which heretofore have been inadequately investigated, or not at all, and (3) ultimate development of a reliable, comprehensive index of the quality of performance of gas-fluidized beds.

In this paper is presented the use of X-ray absorption as a quantitative tool for the study of local phenomena within fluidized as well as static beds. For example, local bed densities, as well as fluctuations thereof, at any level of a fluidized (or static) bed of solids are readily determined by means of X-ray absorption. As a specific illustration of the utility of this tool, the results of a study of the importance of the mode of distribution of gas to a fluidized bed are presented.

In the use of X-ray absorption there are no internal probes to interfere physically with the normal action within a fluidized bed, or to be affected by detrimental internal conditions such as high temperature and corrosion. Application of X-ray absorption is not restricted to materials of low electric conductivity, as, for example, in the case of the capacitometric technique of Morse and Ballou. By means of special features which were specifically designed into the X-ray equipment employed in the present study, semiquantitative interpretation of the data obtained can be made almost instantly (which is especially useful in exploratory experimentation), and thorough interpretation of data can be effected much more rapidly than would be otherwise possible.

The application of X (or gamma)-ray absorption to other chemical engineering studies, such as, studies of liquid holdup and flooding in packed and wetted-wall columns, entrainment studies, etc., is readily conceivable.

ELEMENTS OF X-RAY ABSORPTION*

X-ray absorption has been employed qualitatively and semiquantitatively for the X-ray examination of the human body, for the location of structural imperfections in equipment, etc., since shortly after the discovery of X-rays by Roentgen in 1895. The use of X rays for these purposes was greatly stimulated by the invention of the modern X-ray tube by Coolidge in 1913. Quantitative applications of X-ray absorption, however, became prevalent only about 10 years ago, when for the first time convenient, precise measurement of X-ray intensities was made possible by the development of the phosphor-activated multiplier phototube (*7* and *11*). The latter is the basis of the most sensitive device generally available today for the measurement of X rays and similar high-energy radiation, the scintillation counter.

Following the development of these convenient, precise instru-

*The principles discussed here also apply for the most part to the absorption of gamma rays.

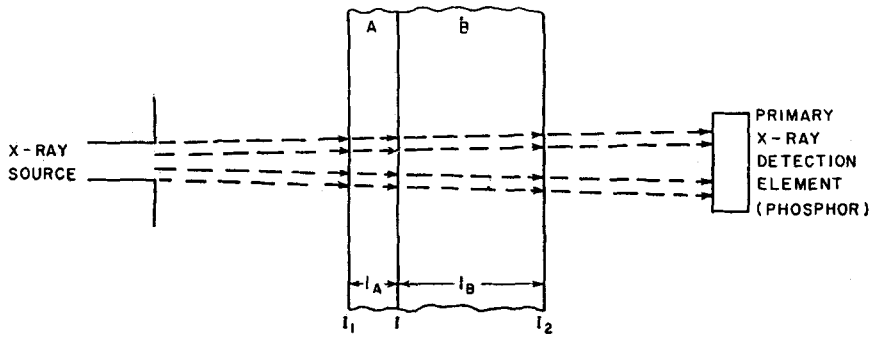

Fig. 1. Schematic diagram for *X*-ray absorption.

ments for the measurement of radiation, extensive applications of X-ray absorption for chemical analysis were made (*4, 5, 6, 9, 12, 17*, and *18*). Indeed, the techniques proposed here for the study of fluidization were developed from many preliminary experiments carried out with the X-ray photometer employed by Smith, Tanis, Liebhafsky, and Winslow in their pioneering quantitative absorption studies (*5* and *11*).

The outstanding characteristic of X rays, from which others derive, is their high energy, or short wave length. Because of this characteristic, the absorption of X rays usually involves only electrons near the atomic nucleus. (The absorption of ultraviolet, visible, or infrared radiation, on the other hand, affects the outer, or valence, electrons, which determine the chemical properties of the elements involved.) X-ray absorption, therefore, which is essentially a process for counting the number, and indicating the kind, of atoms by which the radiation is being absorbed, is virtually independent of the chemical or physical state of the atoms. An oxygen atom per se, for example, will show essentially the same absorption in oxygen gas and in ice, water, steam, and sand.

The absorption of essentially parallel, monochromatic X rays by a homogeneous material of density ρ and thickness l is described by Lambert's law:

$$I = I_o e^{-\mu_m \rho l} \qquad (1)$$

or

$$\ln (I/I_o) = \ln I - \ln I_o = -\mu_m \rho l \qquad (1a)$$

where I_o and I denote the intensities of the incident and transmitted radiation, respectively, and μ_m denotes the mass absorption coefficient of the absorbent. In the application of Equation (1) to a fluidized bed, l becomes the inside diameter of the column and ρ the bulk density of the bed, the variable under study.

The mass absorption coefficient, μ_m, for a given element is independent of the physical state and for chemical compounds is in the first approximation additive from the mass coefficients of the constituent elements. For elements, μ_m depends only upon the wave length of radiation involved; moreover, this dependency is much less complex than for the absorption of radiations of low energy. In the regions of continuous absorption (*1*) most commonly encountered in quantitative X-ray absorption studies, μ_m varies in accordance with the following approximate relationship (*11a*):

$$\mu_m = NCZ^4 \lambda^3/A \qquad (2)$$

where N is Avogadro's number, C is approximately constant in wavelength ranges between adjacent critical absorption wave lengths or "absorption edges," Z is the atomic number, A the atomic weight, and λ the wave length in Angstrom units.

In practice polychromatic X-ray beams are much more frequently employed than monochromatic beams, because they are easier to produce. Equation (1) applies rigorously only to individual monochromatic components of a polychromatic beam, and so for an entire polychromatic beam, use of an integral form of Equation (1) is theoretically required. Fortunately, however, for many practical cases in which polychromatic X radiation is employed, the direct application of Equation (1) serves adequately over the limited ranges of conditions usually encountered.

PRINCIPLES OF X-RAY ABSORPTION APPLIED TO A FLUIDIZED BED

A Pyrex-walled fluidization column was employed in the present study (Figure 3), a simplified representation of which is given in Figure 1. Zone *A* represents the walls of the column, and zone *B* the fluidized (or static) bed. Absorption of the primary radiation by air or by the fluidizing gas is negligible, and consideration of other constant absorbing mediums, such as the protective enclosure of the scintillation crystal, can be included with that of the column walls in zone *A*. For precise work the X-ray beam reaching the phosphor must not be too divergent; otherwise different portions of the beam will have penetrated different thicknesses of the material.* The area of the phosphor should be sufficient to intercept all direct unabsorbed primary radiation, but not so large as to intercept much scattered and background radiation.

Applying Equation (*1a*) to zones *A* and *B* results in

$$\ln I_1 - \ln I = \mu_m^A \rho_A l_A$$

$$\ln I - \ln I_2 = \mu_m \rho_B l_B$$

$$\ln I_1 - \ln I_2 = \mu_m^A \rho_A l_A + \mu_m^B \rho_B l_B$$

$$= \text{"cell constant"} + \mu_m^B \rho_B l_B \qquad (3)$$

If two different absorbers, *B* and *C* (e.g., a fluidized or static bed and a standard thickness of pure aluminum, respectively) produce identical attenuation of a given incident beam (i.e., I_2 as well as I_1 are the same for both cases), the densities and thicknesses of the two absorbers are related by means of Equation (3) as follows:

$$\mu_m^B \rho_B l_B = \mu_m^C \rho_C l_C \qquad (4)$$

$$\rho_B = \frac{\mu_m^C}{\mu_m^B} \frac{\rho_C}{l_B} l_C = K l_C \qquad (4a)$$

$$K = \frac{\mu_m^C}{\mu_m^B} \frac{\rho_C}{l_B} \qquad (4b)$$

$$K = \frac{\rho_B}{l_C} \qquad (4c)$$

*For purpose of simplification of the present discussion, it is assumed that on a time-average basis, the small localized volume of a fluidized bed (or static bed) under examination at a given time is effectively homogeneous: i.e., it is uniformly fluidized (or uniformly packed). This in no way precludes the possibility of gross instantaneous variations in bed densities within a column, as illustrated in later sections of this paper.

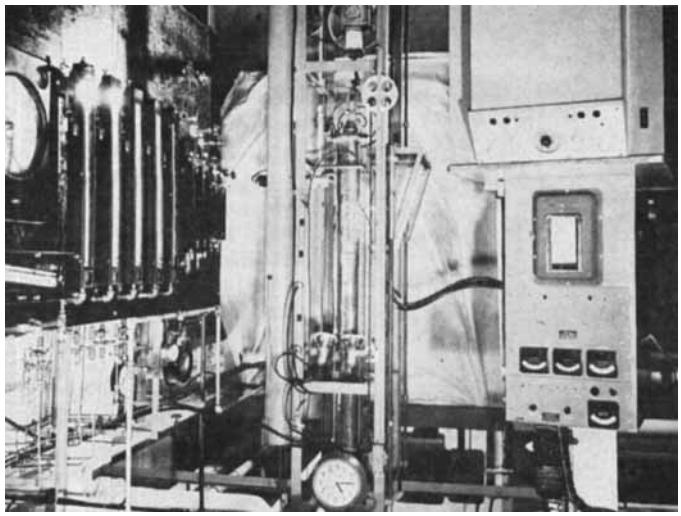

Fig. 2. Over-all view of fluidization apparatus including X-ray photometer.

Equation ($4a$) is the basic equation employed in this study for the determination of local bed densities. For this purpose, l_C becomes the thickness of calibration standard (aluminum) which will produce identical attenuation of the incident beam as produced by a localized volume of bed of bulk density, ρ_B. The quantity l_B becomes the inside diameter of the column.

When, as in the present study, polychromatic radiation is employed, and comparisons between the absorption of X rays by the "unknown" and standard materials, respectively, cannot be made under geometrically identical conditions, it is preferable to determine K empirically, by the use of Equation ($4c$), on standard densities of the actual materials contained in the actual vessel to be employed in the investigation proper (silicon

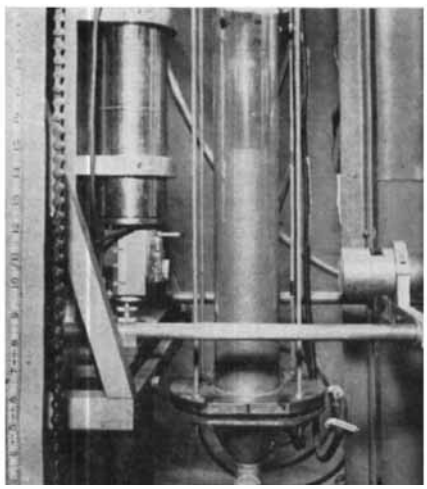

Fig. 3. Close-up of fluidization column showing X-ray source and detection probe.

rates, which adequately covers the ranges of fluidized- as well as fixed-bed operation. Five Meriam well-type manometers measure various pressure differentials, including those produced by the gas distributor, the entire bed, 6-in. sections of the bed, and the cyclone-filter system employed for the collection of entrained fines. A multiple flange arrangement at the bottom of the column permits easy changeover of the gas distributor as well as of the charge of solids. With the flange and pressure-tap arrangement employed, the bottom ¼ in. of the bed is excluded in the measurement of bed pressure differentials and included in the measurement of distributor pressure differentials.

Carryover of solids into manometer lines is effectively prevented by the use of short lengths of ordinary pipe cleaners and/or glass wool

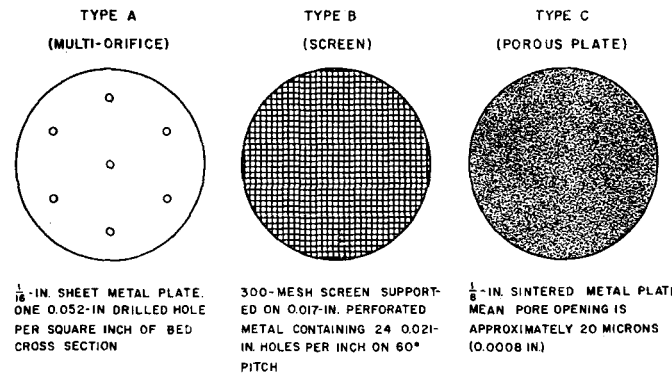

Fig. 4. Gas distributors.

in the Pyrex fluidization column in the present case). In this case standard densities must be known or measurable by means other than X-ray absorption. The application of Equation ($4a$), including the determination of K values, is discussed later.

When absorption comparisons can be made under geometrically identical conditions, it is frequently possible to avoid empirical calibrations through the use of published values of mass absorption coefficients of the elements involved (*1* and *16*).

APPARATUS

An over-all view of the experimental setup is given in Figure 2. The fluidization apparatus proper is relatively conventional, although designed for maximum versatility. The column proper is Pyrex glass, 3.33 in. I.D. This diameter was considered to be about the minimum required in order to avoid excessive "wall effects" and about the maximum with which precise density measurements could be made with relatively low-energy X rays. A bank of five Flowrators provides a 30,000-fold range of gas inserted in the pressure taps. This proved much more satisfactory than the use of "blow-back" devices, which were initially tried.

The unique feature of the present study is the use of the X-ray absorption techniques already discussed. Although believed to be widely applicable to other problems, components of the X-ray photometer employed were specifically designed or selected for the study of fluidization. By means of this photometer, therefore, the action within a fluidized bed can be interpreted in a semiquantitative manner, at least, almost instantly. This is an important advantage in exploratory experimentation. Also, because of the special design features incorporated into the photometer, thorough interpretation of experimental data can be effected much more rapidly than would be otherwise possible.

The X-ray source consists of standard components of the General Electric XRD-3D X-ray diffraction unit with a Machlett AEG-50T tungsten target X-ray tube. The detection equipment consists of a modification of the rate meter in a standard General Electric SPG X-ray detector, fed by a General Electric scintillation probe. The rate-meter response is logarithmic over most of its range

of sensitivity; hence, in accordance with Equation (1*a*), the recorder reading varies approximately linearly with the local bed density being measured. For the purpose of determining instantaneous as well as time-averaged local bed densities, rate-meter time constants ranging from 0.01 to 30 sec. may be employed (*cf.* Figure 8). X-ray intensities are recorded on a General Electric fast-response photoelectric recorder. Details and further discussion of this equipment are given in the Appendix.*

The X-ray tube and radiation probe are mounted on a crank-operated, counterweighted carriage, which can be moved up and down the fluidization column. In this way vertical density traverses of the bed can be made very quickly. The X-ray tube and radiation probe can also be rotated about a vertical axis, by means of which horizontal traverses can be made. Figure 3 shows a close-up of the movable X-ray assembly.

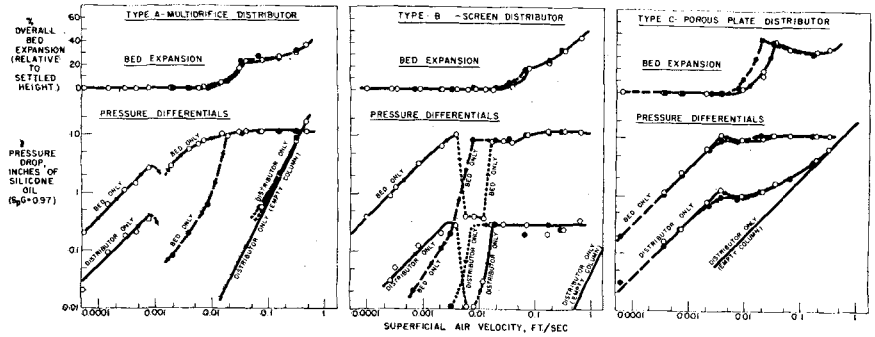

Fig. 5. Bed expansion and pressure differentials: ○, data obtained in order of increasing velocity; ● data obtained in order of decreasing velocity; 3.33 in. I.D. column, 4.0-lb. charge of silicon (all through 200 mesh).

Roller-particle-size Analysis

Micron range	% in range
0—10	2
10—20	8
20—40	34
40—57	50
57—74	4
74	2

BED-EXPANSION AND PRESSURE-DROP STUDIES

Preliminary to the X-ray studies of fluidization, conventional data on bed expansion and pressure drops were obtained in the following manner: 4.00 lb. of commercial silicon powder (all through 200 mesh; *see* Figure 5) was charged through the top flange of the column while a small flow of air was passed through the distributor in cases where the design of the distributor permitted powder to fall through it, i.e., types *A* and *B* of Figure 4. The vent of the column was temporarily closed and the column pressurized with air to about 20 in. of water while a check for gas tightness was made. The bed was expanded and vigorously fluidized for several minutes, then allowed to settle by gradual shutoff of the air flow over a period of at least several minutes. At this point a run was begun.

The lowest practical air velocity obtainable was then applied to the column and maintained for a 3-min. period, following which the total bed expansion and pressure differentials were measured. The flow rate was then increased to a new value and the foregoing procedure repeated. After reaching the maximum velocity for the given run, the entire sequence was repeated in order of decreasing velocity. Figure 5 summarizes the pertinent results for three distinctly different types of gas distributors described in Figure 4.

A of Figure 4 simulates the type of gas distributor frequently employed in commercial fluidization columns. It is designed to produce a reasonably high pressure drop, which ordinarily is required for stable operation of a fluidized column. *B* characterizes the type of distributor frequently employed in laboratory investigations of fluidization (e.g., reference *2*), which offers negligible resistance to gas flow, but tends to produce unstable fluidization. *C* combines the opportunity for uniform gas distribution inherent in the design of *B* with the high pressure drop for operational stability incorporated in the design of *A*.

The distinct superiority of the porous-plate distributor, at least for the single powder composition reported here, appears obvious from Figure 5. Superior bed expansion, for example, is obtained with the porous-plate distributor over the practical range of operating velocities, which is limited by entrainment considerations. Serious gas channeling, visibly obvious during operation with the multiorifice and screen distributors, is graphically indicated by the discontinuities in the pressure-drop curves for these distributors.

The foregoing differences in fluidized-bed performance are even more dramatically brought out by X-ray absorption measurements, as discussed in the following sections.

In Figure 5 pressure differentials across the distributors are shown to be considerably higher when the column is filled with powder than when it is empty, except at the higher gas velocities corresponding to vigorous or violent fluidization. These discrepancies are due partly to the inclusion of the bottom ¼ in. of the bed in the measurement of distributor pressure differentials under filled column conditions (*cf.* p360). From experiments with coarser powders, however, these discrepancies are indicated to be due mainly to obstructions within the gas passages in a distributor caused by the finer particles present in a charge of powder. At sufficiently high velocities these obstructions become largely dispersed.

X-RAY ABSORPTION STUDIES

Preliminary Calibrations

Local bed densities were determined by application of Equation (4*a*) in the following manner:

1. With an incident X-ray beam of the quality* and intensity* employed in the fluidization experiments, the empty column is "calibrated" against a range of standard thicknesses of pure aluminum,† which produces the same range of transmitted intensities as produced by silicon beds in the fluidized as well as unfluidized states. Figure 6 shows a plot of typical results so obtained. Over the thickness range of major interest the plot is essentially a straight line, in accordance with Equation (1*a*). Slight curvatures in Figure 6 are due to (*a*) the use of polychromatic instead of monochromatic X rays, (*b*) deviations from logarithmic amplification at counting rates below around 50 counts/sec. (*cf.* Figure 7), and (*c*) appreciable coincidence counting errors at counting rates exceeding about 1,000 counts/sec. (*E.g.*, at a rate of 2,400 counts/sec. intercepted by the phosphor, the estimated coincidence counting error is approximately 10%.)

2. Detector readings obtained during density-profile determinations were translated into local bed densities by means of Equation (4*a*) as follows: When Equation (4*a*) is ap-

*Copies of the Appendix will be gladly supplied by the author upon request.

*Functions only of the target voltage and emission current for a given X-ray tube.

†Aluminum is particularly suitable as a calibration standard in the present study, since aluminum and silicon differ by only one in atomic number and hence have closely similar X-ray-absorption characteristics.

plied, l_B becomes the inside diameter of the fluidization column and l_C the thickness of calibration standard which will produce identical attenuation of the X-ray beam as produced by a volume of solids of bulk density, ϱ_B. The ratio of the mass absorption coefficients $\mu_m{}^C/\mu_m{}^B$ can be expected to be approximately constant over the range of wave lengths involved, since aluminum and silicon are adjacent in atomic number, and the critical absorption wave lengths for these elements are sufficiently removed from the range of "effective wave lengths" of the polychromatic X-ray beams employed (*1* and *5*). Hence it is to be expected that variations of K under the conditions of the present study would be small, and the local bed densities, therefore, would be approximately proportional to the equivalent thickness of aluminum, l_C.

Values of K as a function of ϱ_B were determined in the identical column employed in the fluidization investigation. The column, equipped with the porous-plate distributor, was charged with 4.00 lb. of silicon powder. (*See* Figure 5 for particle-size analysis.) After a brief initial period of fluidization to homogenize the bed, the gas velocity was reduced to produce bed conditions at which total bed heights could be accurately measured and, hence, average bed densities accurately calculated. Average bed densities were so determined from the charge weight, column cross-sectional area, and total bed height for bed conditions ranging from those for a densely packed bed, through increasing states of expansion, to conditions approximating those for incipient fluidization, (*2* and *14*). As noted in Figure 5, when the porous-plate distributor is employed bed expansion under conditions of incipient fluidization is actually greater than for conditions for active fluidization, within the range of practical air velocities. Hence this technique permitted the determination of K values corresponding to actual densities which may be encountered in a fluidized bed, ranging from the densities of static or stagnant zones to the densities of vigorously fluidized zones.

At each condition of bed expansion transmitted X-ray intensities were measured over the entire bed height. The value of l_C employed in Equation (4*c*) was selected to correspond to the average recorder reading, obtained by integration of a plot of the recorder readings as a function of the bed level. Since over the range of conditions involved, bed density

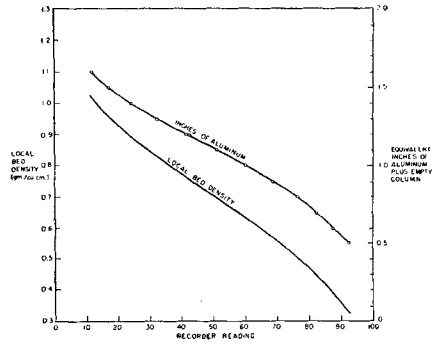

Fig. 6. Typical calibration of X-ray photometer: target voltage, 27,000; emission current, 3 ma.; phototube voltage, 850.

varies essentially linearly with recorder reading, this procedure permitted rigorous evaluation of K values. The eight K values so determined (0.622 to 0.635) varied over a range of only 2%. It is of interest to observe this almost exact agreement with the range of K values (0.620 to 0.635) calculated from literature values of the mass absorption coefficients for pure aluminum and silicon for the energy range of 10 to 30 kv. (*16*). However, this remarkable agreement must be considered at best a coincidence, since significant differences would be expected owing to the small concentrations of elements of higher atomic number present in commercial silicon, such as iron, which have much higher mass absorption coefficients than pure silicon. [*Cf.* Equation (2).]

The density curve in Figure 6 follows directly from Equation (4*a*) upon substitution of the experimentally determined K values.

Probable Error of Density Measurement

In the determination of average local bed densities (Figures 10 and 11) recorder readings taken with a rate-meter time constant of 10 sec. (*cf.* Appendix and Figure 8) and a chart speed of 36 in./hr. were averaged over a period of 1 or 2 min. Maximum and minimum instantaneous local bed densities (Figure 11) were determined by averaging the minimum and maximum recorder readings, respectively, over a period of 5 sec., corresponding on the average to about 25 to 30 cycles of fluctuation of the recorder readings. (*cf.* Figure 8.) For these measurements a time constant of 0.01 sec. and a chart speed of 36 in./min. were employed.

Sample chart records, obtained under typical conditions of vigorous fluidization, are shown in Figure 8 for the entire range of time constants incorporated into the design of the rate meter (*Cf.* Appendix.) The "fast" and "slow" chart speeds correspond, respectively, to 36 in./min. and 36 in./hr.

In X- or gamma-ray absorption some fluctuations in the measurement of transmitted intensities—and hence apparent fluctuations in bed densities—are inherent, even in the measurement of static systems, owing to the random nature of X or gamma radiation.* These random fluctuations, which must be taken into account in the rigorous analysis of radiation measurements made under conditions of fluidization, in order to distinguish between actual and apparent density fluctuations, depend upon the total number of photons, or "counts," recorded by the detector. This number is equal to the product of three factors: transmitted intensity, duration of the intensity measurement, and detection efficiency. In the present study the transmitted intensity is determined by the incident intensity and energy level and the bed density being measured. Duration of intensity measurement is determined by the rate-meter time constant. The detection efficiency is essentially 100%. By proper combination of these factors, random

*Under the conditions employed in this study the random nature of X rays arises chiefly from the randomness of the electron emission from the X-ray tube filament as well as from the random nature of the atomic excitation process which results in the emission of the X rays.

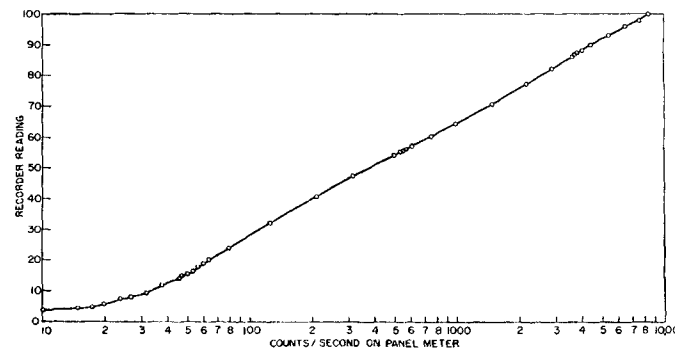

Fig. 7. Relationship between recorder reading and counting rate.

fluctuations in transmitted intensities—and, hence, in bed densities—can be made negligible.

For the X-ray conditions generally employed in this study, random fluctuations in bed density, as a function of actual bed density being measured and rate-meter time constant, are given in Figure 9 by the vertical distances between pairs of curves labeled with the same time constant. For example, if at a given moment the true density of a zone of the bed were 0.75 g./cc., the probable instantaneous density measurement, employing a time constant of 0.01 sec., would range from approximately 0.72 g./cc. minimum to 0.79 g./cc. maximum. Figure 9 was constructed from X-ray measurements taken with various time constants on thicknesses of aluminum equivalent to the bed densities given by the data points. The ranges of fluctuation given in Figure 9 were obtained by averaging the maximum and minimum recorder readings over a suitable time interval (e.g., 1 or 2 min. for the 10-sec. time constant and about 5 sec. for the 0.01-sec. time constant).

Under conditions of the present study random fluctuations in the measurement of average local bed densities, determined with the 10-sec. time constant, were negligible. On the other hand, instantaneous local bed densities, which were determined with the 0.01-sec. time constant, were subject to the following probable errors of measurement due to random fluctuations (approximated from Figure 9):

True instantaneous bed density, g./cc.	Approximate probable Error of measurement, % Positive	Negative
0.70	3	3
0.75*	5	4
0.8	8	6
0.9†	20	7
1.0	30	10

*Approximate density corresponding to "incipient fluidization."

†Approximate settled bed density with porous-plate distributor.

Under most conditions of active fluidization encountered in this study, therefore, the probable errors of measurement of instantaneous bed densities were not excessive.

Increased precision of measurement of higher bed densities for a given time constant is readily attained by the use of an increased target voltage, hence, an increased transmitted intensity.

Bed-Density Profiles

In Figure 10 profiles of time-averaged local bed densities, as functions of gas velocity, are given for the three gas distributors previously discussed. All the results apply to the single powder composition given in Figure 5. The corresponding instantaneous bed density profiles, along with the time-averaged density profiles for comparison, are given in Figure 11.

As a check of the reliability of the time-averaged density profiles, these were integrated over the entire bed height in order to obtain length-average bed densities which could be compared with the corresponding values calculated from the weight of powder charged and the total bed height. Under settled bed conditions and at an air velocity of 0.05 ft./sec., corresponding values of length-average bed density agreed within 3% or better. At velocities of 0.15 and 0.25 ft./sec. it was difficult to measure total bed heights accurately, because of excessive turbulence of the menisci, and discrepancies as great as 9% (and in one case 15% with the multiorifice distributor at 0.25 ft./sec.) were noted.

Before any further discussion of Figures 10 and 11, it is of interest to report the results of an auxiliary series of experiments. In this

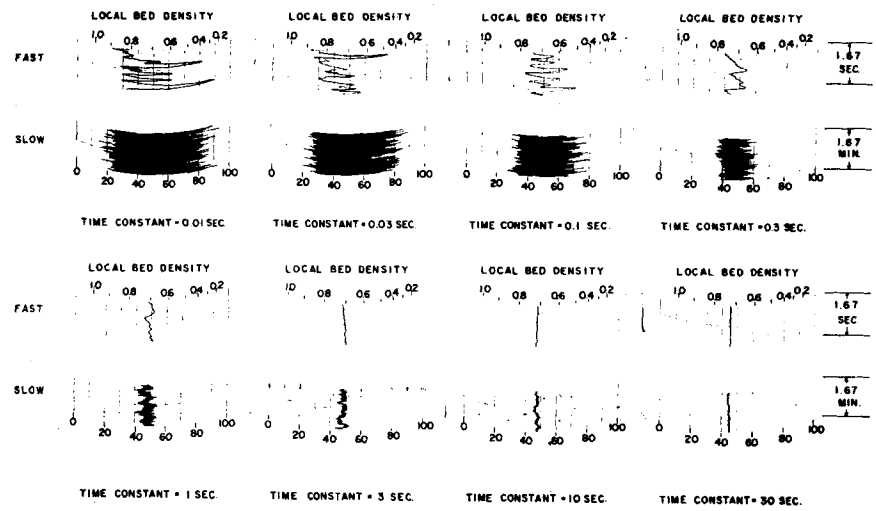

Fig. 8. Sample of *X*-ray absorption measurements of fluid-bed performance.

GAS DISTRIBUTOR ..... TYPE B
SUPERFICIAL AIR VELOCITY ..... 0.15 FT./SEC.
DISTANCE ABOVE DISTRIBUTOR ..... 12½ IN.
TOTAL FLUIDIZED-BED HEIGHT ..... APPROX. 15 IN.

TARGET VOLTAGE 27000
EMISSION CURRENT ..... 30 ma.
PHOTO-TUBE VOLTAGE 1000

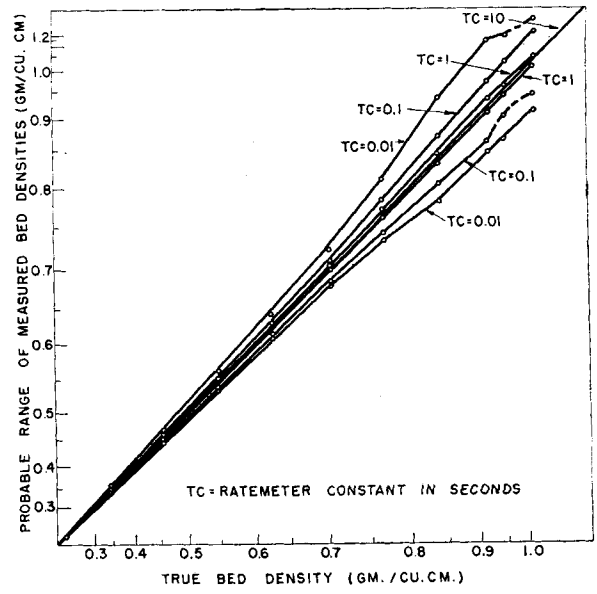

Fig. 9. Apparent fluctuations in bed density due to random fluctuations in the measurement of transmitted radiation intensities.

series the air flow (0.15 ft./sec.) to a vigorously fluidized bed,* employing the porous-plate distributor, was abruptly terminated, and the resulting settling of the bed, with corresponding increased bed densities, was followed by X-ray absorption. A time constant of 0.01 sec. and chart speed of 36 in./min. were employed. The procedure was repeated at various levels of the bed up to the 12-in. level. After an initial rapid increase in bed density immediately following gas shutoff, a distinct leveling off, or "plateau," in the density-time curve was observed, before final settling of the bed began. The duration of these plateaus, ranging from 1 to 15 sec., varied roughly linearly with bed level. The "plateau bed densities" so obtained were essentially constant at 0.74 ± 0.01 g./cc.

The foregoing results follow logically from the fact that upon termination of gas flow to a fluidized bed, collapse or settling of the bed obviously must progress upward from the distributor, and partial expansion of the upper zones of the bed is therefore maintained by the gas liberated from the lower zones of the bed for periods of time roughly proportional to the bed level under consideration.

As postulated by a number of investigators, the general gas-fluidized system includes two "phases": a continuous phase, consisting of uniformly distributed particles in a supporting gas stream, and a discontinuous phase, consisting of essentially solids-free gas, which may pass through the bed in the form of bubbles, channels, or slugs. This is "two-phase" or "aggregative" fluidization. A bed of solids fluidizes when the superficial gas velocity is sufficient to support the particles; this is the point of "incipient" fluidization. At appreciably higher gas velocities, a discontinuous phase appears and imparts convective motion to the continuous phase to produce "aggregative" fluidization. For certain gas-solid systems it may be possible for "single-phase" or "particulate" fluidization to exist over a short range of velocities exceeding that required for incipient fluidization, without the appearance of a second, discontinuous phase. Toomey and Johnstone (*13*) postulate that the appearance of the discontinuous phase imposes no significant changes upon the physical character of the continuous phase; e.g., the voidage or density of the continuous phase and the interstitial velocity remain essentially constant, independent of increasing superficial velocities. The latter is doubtless an oversimplified concept, although very useful for promoting clearer understanding of the mechanism of gas fluidization.

The essentially constant plateau bed density reported above is believed to correspond closely to the condition of incipient fluidization.

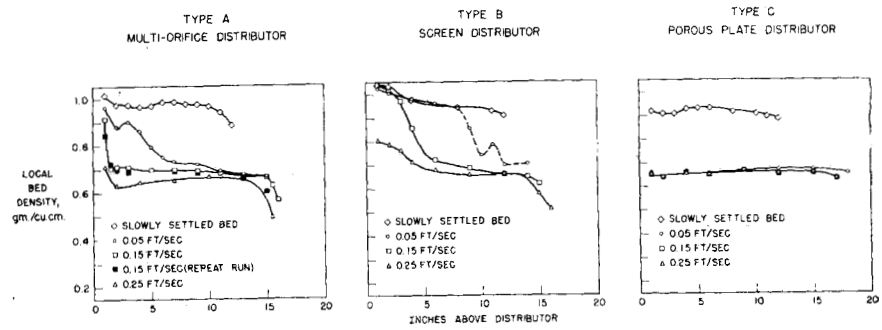

Fig. 10. Average bed-density profiles. 3.33 in. I.D. column; 4.0-lb. charge of silicon (see Figure 5 for particle-size analysis); target voltage: settled-bed data, 31,000, all other data, 27,000; emission current, 3.0 ma.; phototube voltage, 850; time constant, 10 sec.

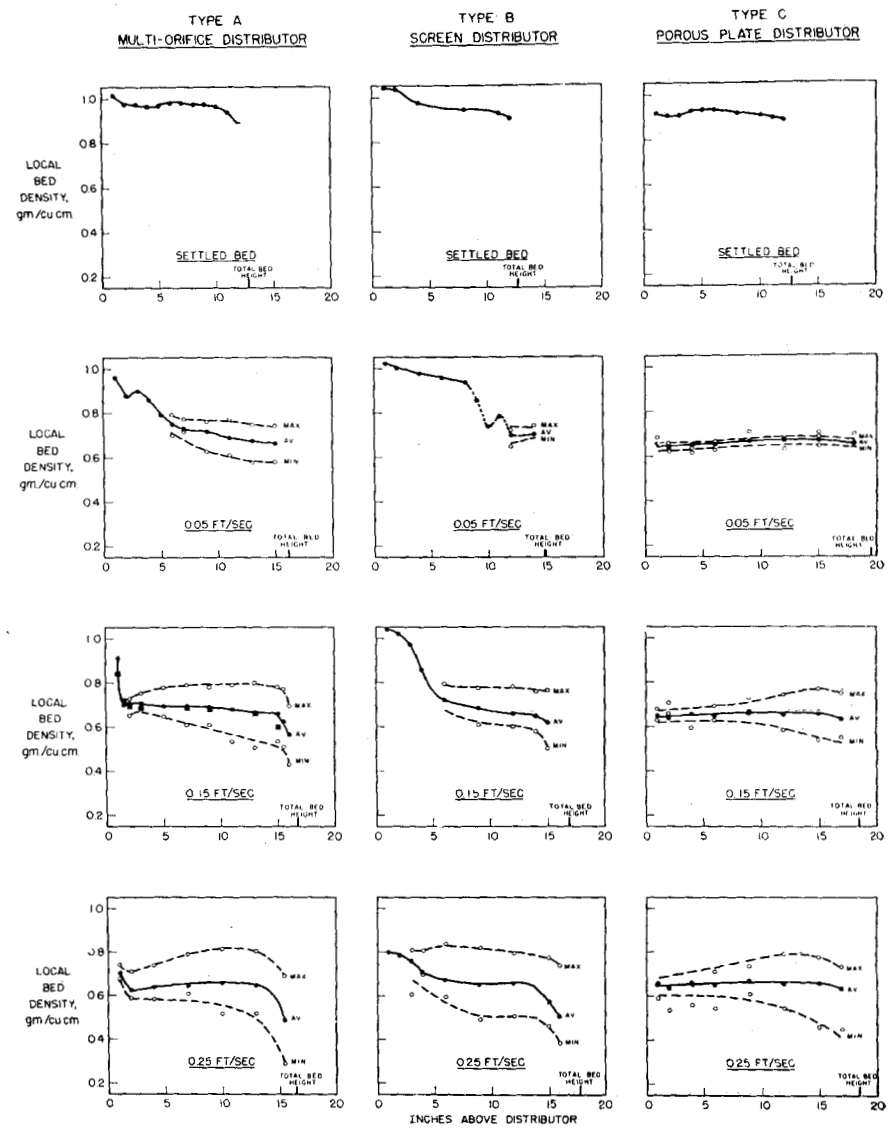

Fig. 11. Instantaneous bed-density profiles (same data as in Figure 10 except for time constant, which is 0.01 sec. for instantaneous densities and 10 sec. for average densities).

Applying the value 0.74 g./cc. for the incipient fluidization density to the total bed-expansion data given for the porous-plate distributor in Figure 5 enables the incipient fluidization air velocity to be estimated at approximately 0.030 ft./sec. if arrived at from a lower velocity and 0.017 ft./sec. if arrived at from a higher velocity. Also, from the porous-plate-bed-expansion data, along with visual observations, the transition between particulate and aggregative fluidization (i.e., the condition of maximum bed expansion without more than intermittent appearance of appreciable gas bubbling) was estimated to occur at a length-average bed density of 0.64 g./cc. and a superficial air velocity of 0.035 ft./sec. if arrived at from a lower velocity and 0.020 ft./sec. if arrived at from a higher velocity. Hence 0.030 to 0.035 ft./sec. and 0.017 to 0.020 ft./sec., arrived at from a lower and higher velocity, respectively, represent the approximate velocity ranges at which particulate fluidization occurs for the given combination of powder and gas properties, column design, and gas distributor design. There was no evidence that particulate fluidization could even be approximated with either the multiorifice or screen distributors.

Local bed densities (Figures 10 and 11) greater than 0.74 g./cc. (i.e., greater than the incipient fluidization density) are indicative of completely or periodically stagnant zones within the bed. In a fluidized reactor stagnant bed conditions would give opportunity for hot spots, tar formation, deactivation of catalyst, powder caking and gas channeling to occur. On the other hand, densities appreciably less than 0.64 g./cc. indicate zones in which an appreciable, and frequently a major, proportion of the incoming gas flow is short-circuiting the bed. Actually it is possible for short-circuiting of the gas flow to occur within zones of the bed possessing densities exceeding 0.64 g./cc., or even within stagnant beds, when gas channeling or intermittent compression of the continuous phase takes place.

The distinct superiority and inferiority, respectively, of the porous-plate and screen* distributors, previously indicated by the bed-expansion and pressure-drop experiments, are emphasized by the X-ray absorption studies. Over the entire range of bed levels possible to probe accurately with the X-ray photometer (to within about an inch from the bottom or from the top of the bed), extremely uniform average bed-density profiles are shown for the porous-plate distributor, even at the lowest gas velocity reported (0.05 ft./sec.). On the other hand, results for the screen distributor exhibit appreciable nonuniformities of the bed at the highest velocity reported (above which entrainment losses become objectionably high) and extremely nonuniform, incomplete, and erratic fluidization at the lower velocities. Performance data for the multiorifice distributor again fall intermediate in quality, compared with those for the porous-plate and screen distributors.

It is of interest to note that the screen distributor employed in the present study, described in Figure 4, is essentially identical in design to that employed by Lewis, Gilliland, and Bauer for the fluidization of Scotchlite glass beads (*3*). Whereas particularly poor performance was obtained with the screen distributor in the present study of the fluidization of silicon, no mention of similar performance deficiencies was made by Lewis et al. The apparent differences in performance are believed likely attributable to inherently different fluidizing characteristics of Scotchlite beads, which are quite round and smooth, and silicon powders, which are of a sharp, gritty nature. It is planned to investigate this apparent anomaly by fluidization of Scotchlite beads in the present apparatus.

Stagnant zones of powder were clearly visible in the operations with the screen and multiorifice distributors. Even with the porous-plate distributor, a small amount of powder inactivity could be observed immediately adjacent to the distributor. In the latter case, however, this is believed likely to have been simply a small "wall" or "corner" effect, extending for only a very short distance above the distributor.

Powder-packing tendencies, which give rise to stagnant zones in fluidized beds, are further indicated by the settled bed-density profiles for the screen and multiorifice distributors. They are less uniform and include appreciably higher densities than in the case of the porous-plate distributor.

Operation of the porous-plate distributor at 0.05 ft./sec. is shown in Figure 11 to be the only case in which the instantaneous bed densities all fell closely within the range corresponding to particulate fluidization, 0.64 to 0.74 g./cc., and, indeed, from visual observations fluidization appeared most uniform under these conditions.

*Same charge and particle-size analysis as employed in the density-profile determinations.

CONCLUSION

Reported above is a preliminary interpretation of the results of the X-ray absorption studies of fluidization. More thorough analysis of such results can be shown to lead to an improved understanding of the mechanism of gas fluidization. Such an analysis, based upon additional experimentation, including the use of high-speed movies, is currently in progress.

LITERATURE CITED

1. Compton, A. H., and S. K. Allison, "X-Rays in Theory and Experiment," 2 ed., D. Van Nostrand Co., Inc., New York (1935).
2. Leva, M. et al., *U.S. Bur. Mines, Bull.* 504 (1951).
3. Lewis, W. K., E. R. Gilliland, and W. C. Bauer, *Ind. Eng. Chem.*, 41, 1104 (1949).
4. Liebhafsky, H. A., and E. H. Winslow, *Gen. Elec. Rev.*, 48, 36 (April, 1945).
5. Liebhafsky, H. A., H. M. Smith, H. E. Tanis, and E. H. Winslow, *Anal. Chem.*, 19, 861 (1947).
6. Liebhafsky, H. A., Ann. N. Y. Acad. Sci., 53, 997 (1951).
7. Morgan, R. H., *Am. J. Roentgenol. Radium Therapy, Nuclear Med.*, 48, 88 (1942).
8. Morse, R. D., and C. O. Ballou, *Chem. Eng. Progr.*, 47, 199 (1951).
9. Rich, T. A., and P. C. Michel, *Gen. Elec. Rev.*, 50, 45 (February, 1947).
10. Shuster, W. W., and P. Kisliak, *Chem. Eng. Progr.*, 48, 455 (1952).
11. Smith, H. M., *Gen. Elec. Rev.*, 48, 13 (March, 1945).

11a. Sproull, W. T., "X-Rays in Practice," McGraw-Hill Book Company, Inc., New York (1946).

12. Titus, A. C., paper presented at A.I.E.E. meeting (1954).
13. Toomey, R. D., and H. F. Johnstone, *Chem. Eng. Progr.*, 48, 220 (1952).
14. ——— *Chem. Eng. Progr. Symposium Series* No. 5, 51, (1953).
15. Weltmann, R. N., and P. W. Kuhns, *Natl. Advisory Comm. Aeronaut. Tech. Note* 2580 (1951).
16. White, G. R., *Natl. Bur. Standards Rept.* 1003 (1952).
17. Winslow, E. H., H. M. Smith, H. E. Tanis, and H. A. Liebhafsky, *Anal. Chem.*, 19, 866 (1947).
18. Zemany, P. D., E. H. Winslow, G. S. Poellmitz, and H. A. Liebhafsky, *loc. cit.*, 21, 493 (1949).